ELSEVIER

Chemical Engineering Journal 78 (2000) 179–185

Chemical Engineering Journal

www.elsevier.com/locate/cej

Measurement and calculation of liquid–liquid equilibria of binary aqueous polymer solutions

Wei Li, Zi-Qiang Zhu*, Mian Li

Department of Chemical Engineering, Zhejiang University, Hangzhou 310027, PR China

Received 9 December 1998; received in revised form 22 October 1999; accepted 22 October 1999

Abstract

The liquid–liquid equilibria (LLE) of aqueous solutions containing random copolymers of ethylene oxide (EO) and propylene oxide (PO) with two different molecular weights were measured. The modified non-random two-liquid (NRTL) model was used to calculate the phase behaviour of water–polymer systems with various molar ratios of EO to PO. Good agreement was obtained with the experimental data. The results show that the molecular weight and the molar ratio of EO to PO of the polymer can strongly influence the phase behaviour of H_2O–EOPO systems. © 2000 Published by Elsevier Science S.A.

Keywords: Liquid–liquid equilibria; Model; Polymer solution; Ethylene oxide and propylene oxide; Cloud-point; Binodal; Spinodal

1. Introduction

Aqueous two-phase systems (ATPSs) are widely used for the separation and purification of biomolecules. The most frequently used two-phase systems are aqueous solution of polyethylene glycol (PEG) and dextran or PEG and potassium phosphate [1,2]. One problem encountered with these systems is the difficulty in separating target biomolecules from the polymer solution. These systems are more cost-effective if the polymer can be readily recycled without costly ultrafiltration or the use of chromatography steps. Recently, a method of temperature-induced phase separation combined with ATPSs has been introduced for the separation and purification of biomolecules in ATPSs [3–6]. This method has proved to offer an effective solution to the problems of polymer removal and recycling. A random copolymer of ethylene oxide and propylene oxide (EOPO) can be used to bring about temperature-induced phase separation.

The complexity of phase behaviour in binary polymer solutions is well known. The temperature–composition phase diagrams usually show a lower critical solution temperature (LCST) or an upper critical solution temperature (UCST). Some systems, which exhibit a miscibility loop, have both LCST and UCST [7,8]. Compared to other phase-forming polymers, EOPO has a relatively lower LCST in water. Below the LCST, the solution is a one-phase system. If the one-phase solution is heated until it reaches the critical solution temperature, the solution becomes cloudy. The temperature at which this phenomenon occurs is called the cloud-point of the polymer. UCON 50-HB-5100, a random copolymer with 50% EO and 50% PO (M_w=4000), has a cloud-point at 50°C (323 K) in water [9]. The cloud-point depends on the structure, the molecular weight and the concentration of polymer, and the addition of solutes with different hydrophobicities [9,10]. The magnitude of the cloud-point can be altered by varying the ratio of EO to PO groups [11]. If the temperature of the polymer solution is increased further, the solution separates into two clearly distinctive phases. The upper phase (usually) contains most of the solvent with very little polymer, while the bottom phase contains part of the solvent with most of the polymer [12]. The point where the concentration and the temperature correspond to the lowest cloud-point is defined as the LCST. Other typical examples with LCST include the aqueous solution of poly(ethylene oxide) (PEO) [10], poly(propylene oxide) (PPO) [13], and Triton X-114 [14].

A large amount of work has been done in an attempt to understand the mechanism of phase separation for water–PEO systems. However, as far as we know, there is a paucity of research reports on the binary liquid–liquid equilibria (LLE) of water–EOPO systems. Application of temperature-induced phase separation combined with ATPS is limited. Furthermore, phase diagrams data are necessary for the development of models that are capable of predicting

* Corresponding author. Tel.: +86-571-7951982; fax: +86-571-7951358.
E-mail address: zhuzq@che.zju.edu.cn (Z.-Q. Zhu)

1385-8947/00/$ – see front matter
PII: S1385-8947(00)00137-6

Table 1
Experimental LLE data of H_2O–EOPO systems

No.	H_2O–EOPO4000			H_2O–EOPO2000		
	T (K)	Concentration of EOPO (w/w)		T (K)	Concentration of EOPO (w/w)	
		Top phase	Bottom phase		Top phase	Bottom phase
1	328.85	18.76	61.51	341.35	18.70	61.24
2	332.55	12.75	65.31	345.25	10.87	65.92
3	339.05	5.30	69.92	350.65	7.10	69.42
4	343.30	3.20	73.94	357.95	4.24	73.73
5	347.20	2.10	76.85	364.65	3.15	75.28
6	352.15	1.40	78.81	373.15	2.16	76.54
7	356.85	1.01	80.75			
8	363.35	0.79	83.15			
9	373.15	0.84	84.61			

phase separation. Thus, the LLE of water–EOPO systems were measured in this study. The modified non-random two-liquid (NRTL) model proposed by our research group [15] has been used to calculate the phase equilibria of water–polymer systems. The polymer components are EOPO (this work), PEO [10] and PPO [13], respectively.

2. Experimental

2.1. Materials

EOPO4000 and EOPO2000 were obtained from Zhejiang University Chemical Factory, PR China. The average molecular weight and the molecular weight distribution of EOPO were determined by gel permeation chromatography (GPC, Waters 150C). Three-column systems (Ultrastyragel linear, 500A and 100A) were used with the column temperature set at 30°C. The solvent was tetrahydrofuran and the flow rate was 1.0 ml/min. The number-average molecular weights (M_n) of EOPO4000 and EOPO2000 were 3640 and 2340, respectively. The polydispersities of EOPO4000 and EOPO2000 were 1.1095 and 1.0611, respectively. The EOPO samples used in this work have an equal molar number of ethylene oxide (EO) and propylene oxide (PO). Double-distilled water was used in all water solutions.

2.2. Method

The initial solution contained 20% (w/w) EOPO, and the total weight of the system was 10 g. After the solution was mixed effectively in a test tube, it was placed in a well-stirred water bath for 2 h (separation was completed within 1 h) in order to reach proper phase separation. The cloud-point temperature of a system was determined by heating the sample in a water bath. The cloud-point temperature was defined as the temperature at the time when the sample was visually observed to start to get cloudy. The clouding was closely followed by a macroscopic phase separation.

Phase separation and equilibration were performed over the cloud-point temperature of the system. Phase diagrams were obtained by analyzing the composition of the upper and lower phases at each temperature. The concentration of water was determined by a vacuum-drying method at 65°C for 24 h until the samples had reached constant weight. The concentration of EOPO was calculated by the difference of the concentration of water.

2.3. Experimental results

The cloud-point temperature of 20% (w/w) H_2O–EOPO-4000 and H_2O–EOPO2000 are 324.85 and 338.25 K, respectively. The results show that the cloud-point temperature decreases with an increase in the molecular weight of EOPO. The copolymer EOPO4000 (M_w=4038) used in this experiment has a molecular weight approximately equal to that of UCON 50-HB-5100 (M_w=4000), and both of them have the same ratio of EO to PO. Thus, it can be found that the cloud-point temperature of H_2O–EOPO4000 is approximately equal to that of H_2O–UCON 50-HB-5100 (323 K).

The experimental data of LLE for H_2O–EOPO4000 and H_2O–EOPO2000 systems are given in Table 1. The temperature–composition phase diagram is shown in Fig. 1.

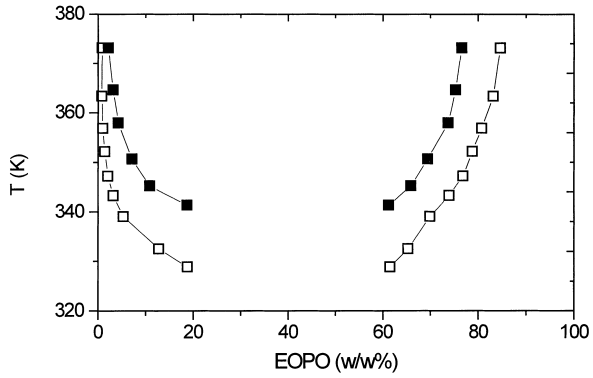

Fig. 1. Experimental temperature–composition phase diagram for H_2O–EOPO: (□) EOPO4000; (■) EOPO2000.

With an increase in temperature, the difference between the concentration of EOPO in the two phases also increases. For example, the upper phase is almost only water and there is very little EOPO at 373 K, while the bottom phase contains most of the EOPO. From the above results, it may be said that the phase composition is strongly influenced by the molecular weight of the polymer. Lowering of the molecular weight causes the binodal curve to go upwards with the two-phase region getting reduced.

3. Theoretical model

In the past several decades, significant efforts have been made in polymer solution theory, beginning with the classical Flory–Huggins model [16,17]. However, it has been known for many years that the Flory–Huggins theory for a close-packed lattice is not able to describe LCST behaviour. Later, many improvements have been made based on the Flory–Huggins theory [18–20]. These theories can be used to describe a phase diagram with both LCST and UCST. However, it must be pointed out that quantitative agreement is far from being satisfactory. In recent years, some thermodynamic models, which can be used to adequately describe phase behaviour including both LCST and UCST, have been proposed for polymer solutions [21–23].

In our previous paper, a modified NRTL equation was developed for the calculation of phase equilibrium of a binary polymer solution [15]. A simple temperature dependence of the model parameters is introduced to account for the oriented interactions without changing the general formulation of the free energy of mixing. The present model is expected to provide a flexible thermodynamic framework for both correlating and predicting the phase equilibrium of polymer solutions.

Based on our previous work, the Helmholtz free energy of mixing, ΔA, can be expressed as follows:

$$\frac{\Delta A}{N_r kT} = \frac{\phi_1}{r_1}\ln\phi_1 + \frac{\phi_2}{r_2}\ln\phi_2 + \alpha\left(\frac{1}{r_1}-\frac{1}{r_2}\right)^2\phi_1\phi_2 + \frac{N_q}{N_r}X_1X_2\left(\frac{\tau_{21}G_{21}}{X_1+X_2G_{21}} + \frac{\tau_{12}G_{12}}{X_2+X_1G_{12}}\right) \quad (1)$$

where

$$N_r = N_1r_1 + N_2r_2, \qquad \phi_1 = \frac{N_1r_1}{N_r}, \qquad \phi_2 = 1-\phi_1,$$

and N_1 and N_2 refer to the molecule numbers of solvent (1) and polymer (2).

$$G_{21} = \exp(-\alpha\tau_{21}), \qquad G_{12} = \exp(-\alpha\tau_{12})$$

where τ is the energy parameter and has meanings similar to the NRTL model.

X_i is the effective mole fraction of the segment of species i:

$$X_1 = \frac{N_1q_1}{N_q}, \qquad X_2 = 1-X_1, \qquad N_q = N_1q_1 + N_2q_2,$$

where q_i is an effective segment number of species i, and may be correlated to r_i as is done in a usual way:

$$q_i = r_i\left[1-2\alpha\left(1-\frac{1}{r_i}\right)\right]$$

The activity of solvent in the system can be derived from Eq. (1):

$$\ln a_1 = \ln\phi_1 + \left(1-\frac{r_1}{r_2}\right)\phi_2 + \alpha r_1\left(\frac{1}{r_1}-\frac{1}{r_2}\right)^2\phi_2^2 + q_1X_2^2\left[\frac{\tau_{21}G_{21}^2}{(X_1+X_2G_{21})^2} + \frac{\tau_{12}G_{12}}{(X_2+X_1G_{12})^2}\right] \quad (2)$$

The non-random factor α is a structural factor of solution and is assumed to be independent of temperature and composition. The value of α falls typically within a range of 0–0.4, and should be carefully selected for different kinds of solutions. At that moment, the general rule proposed in the NRTL model may be used, or α should be fitted to the experimental data.

Considering oriented interactions, the interaction parameters τ can be expressed as follows:

$$\tau_{ji} = a_{ji}^{(1)}\left(\frac{T_0}{T}\right) + a_{ji}^{(2)}\left(\frac{T_0}{T}\right)^2 \quad (3a)$$

$$\tau_{ij} = a_{ij}^{(1)}\left(\frac{T_0}{T}\right) + a_{ij}^{(2)}\left(\frac{T_0}{T}\right)^2 \quad (3b)$$

where T_0 is the reference temperature, T_0=298.15 K, and the adjustable model parameters $a^{(1)}$ and $a^{(2)}$ are assumed to be independent of temperature and composition.

The vapor–liquid equilibrium (VLE) of a homologous polymer solution can be correlated using the above-mentioned modified NRTL model. Good agreement with the experimental data was obtained. Some LLE of polymer solution systems were also calculated. However, to calculate LLE of the system with both UCST and LCST seems to be difficult [15].

As for the description of systems with strong and local interactions, especially for the calculation of the water–polymer systems with both UCST and LCST, a new adjustable parameter c_r is introduced. The adjustable parameter of c_r is defined as follows:

$$c_r = \frac{r_2}{r_2^0} \quad (4)$$

where r_2^0 is the number of segments of polymer, and r_2 the site-occupancy number per molecule of polymer based on r_1=1. Therefore, Eqs. (1) and (2) can be rewritten as

$$\frac{\Delta A}{N_r kT} = \phi_1 \ln \phi_1 + \frac{\phi_2}{c_r r_2^0} \ln \phi_2 + \alpha \left(\frac{1}{r_1} - \frac{1}{c_r r_2^0} \right)^2 \phi_1 \phi_2 + \frac{N_q}{N_r} X_1 X_2 \left(\frac{\tau_{21} G_{21}}{X_1 + X_2 G_{21}} + \frac{\tau_{12} G_{12}}{X_2 + X_1 G_{12}} \right) \quad (5)$$

$$\ln a_1 = \ln \phi_1 + \left(1 - \frac{1}{c_r r_2^0} \right) \phi_2 + \alpha r_1 \left(1 - \frac{1}{c_r r_2^0} \right)^2 \phi_2^2 + q_1 X_2^2 \left[\frac{\tau_{21} G_{21}^2}{(X_1 + X_2 G_{21})^2} + \frac{\tau_{12} G_{12}}{(X_2 + X_1 G_{12})^2} \right] \quad (6)$$

Thus, Eqs. (5) and (6) are our working equations.

The need for c_r arises because the lattice model provides only an approximation for polymer solutions. The solvent molecule can hardly be considered as a spherical monomer, and the polymer molecule is not an ideal flexible chain as has been assumed in the previous theory.

4. Calculation results and discussion

The condition for LLE is the equality of component activities in both phases. The spinodal curve lies inside the binodal, representing the limits of metastable composition, and thus, it is given by

$$\frac{\partial^2 (\Delta A/(N_r kT))}{\partial \phi_1^2} = 0 \quad (7)$$

The spinodal and the binodal meet at the critical point where

$$\frac{\partial^2 (\Delta A/(N_r kT))}{\partial \phi_1^2} = \frac{\partial^3 (\Delta A/(N_r kT))}{\partial \phi_1^3} = 0 \quad (8)$$

In the calculation, the pure-substance parameters r_2^0 are obtained from number-average molecular weight (M_n). The non-random factor, α, is not treated as an adjustable parameter, but is a previously selected one. The other parameters are fitted to the experimental data of two tie lines, and are shown in Table 2. The phase diagrams of three types of water–polymer systems are calculated using the parameters obtained above, and are shown in Figs. 2–6.

Figs. 2 and 3 show the calculated results of H_2O–EOPO-2000 and H_2O–EOPO4000 systems. The calculated binodals are in excellent agreement with the experimental data. The average relative deviation (ARD) values are 1.02 and 2.01% for EOPO2000 and EOPO4000, respectively. The LCST of EOPO2000 and EOPO4000 are calculated to be at 337.63 K (32.22% (w/w)) and 325.37 K (34.96% (w/w)). The calculated UCST of EOPO2000 and EOPO4000 are 426.41 K (41.03% (w/w)) and 459.59 K (37.79% (w/w)). It can be

Table 2
The values of model parameters (α=0.25)

Systems	$a_{12}^{(1)}$	$a_{21}^{(1)}$	$a_{12}^{(2)}$	$a_{21}^{(2)}$	c_r
H_2O–EOPO4000	17.3751	−3.6543	−16.4557	−57.1158	5.9728
H_2O–EOPO2000	27.0791	−10.6852	−27.9140	−39.6716	6.4991
H_2O–PEO2270	5.6990	0.6412	−5.8704	−0.0815	1.6399
H_2O–PEO2180	5.5246	0.6766	−5.7801	−0.0925	1.4786
H_2O–PPO400	27.6703	−12.3769	−27.6114	−37.6071	8.3529

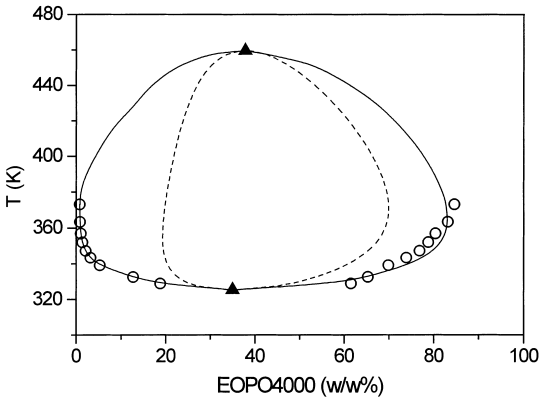

Fig. 2. Phase diagram for H_2O–EOPO4000 (M_n=3640, r_2^0=177.5): (—) calculated binodal; (---) calculated spinodal; (○) experimental data; (▲) calculated critical point.

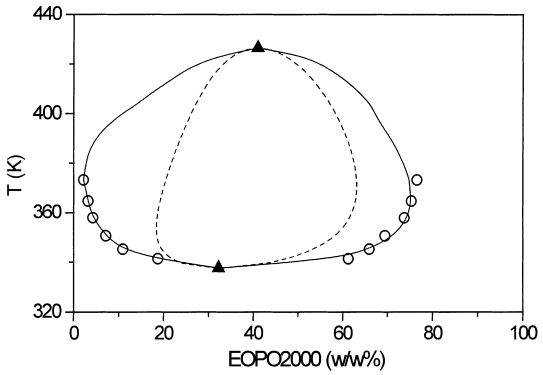

Fig. 3. Phase diagram for H_2O–EOPO2000 (M_n=2340, r_2^0=115): (—) calculated binodal; (---) calculated spinodal; (○) experimental data; (▲) calculated critical point.

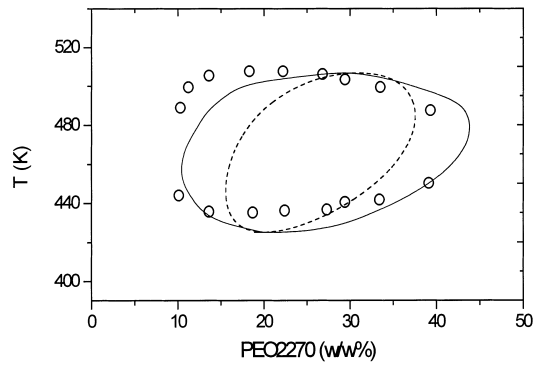

Fig. 4. Phase diagram for H_2O–PEO2270 (M_n=2270, r_2^0=102.4): (—) calculated binodal; (---) calculated spinodal; (○) experimental points — from Sakei et al. [10].

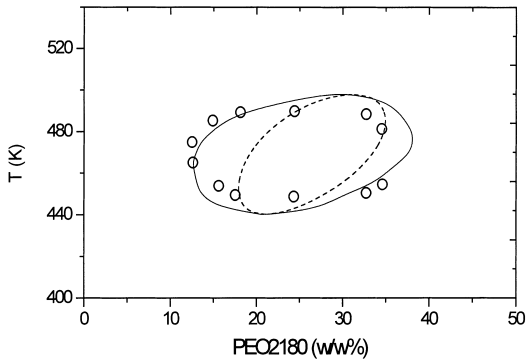

Fig. 5. Phase diagram for H_2O–PEO2180 (M_n=2180, r_2^0=98.5): (—) calculated binodal; (---) calculated spinodal; (○) experimental points — from Sakei et al. [10].

found from Figs. 2 and 3 that the spinodal and the binodal meet at the critical point. With an increase in polymer molecular weight, the difference between LCST and UCST of the water–EOPO system increases. It seems difficult to obtain the experimental data of LLE when the temperature is over 373.15 K. Therefore, the calculated results (over 373.15 K) cannot be compared with the experimental data.

Figs. 4 and 5 show the results of H_2O–PEO2180 and H_2O–PEO2270 systems. The experimental data are obtained from Sakei et al. [10]. Compared to the H_2O–EOPO system, a relatively large deviation arises between the calculated binodals and the experimental data. The experimental LLE data from Sakei were obtained by determining the cloud-point of the system. However, the upper- and the lower-phase composition at a constant temperature after phase separation should be real LLE data. The slight difference between the two methods results in the deviation of calculation being larger. Furthermore, polymers are polydispersive in general; the cloud-point data of the system are influenced by the distributions of the molecular weight for the polymer. As the broadness of the molecular weight distributions of the polydisperse polymer increases, the cloud-point curve is far removed from the binodal curve that reflects phase equilibrium. In this work, the broadness of the molecular weight distributions of EOPO4000 and EOPO2000 is small. Unfortunately, there are no published reports on the polydispersivity for the polymers used in Sakei's experiments. Thus, it is difficult for us to definitely confirm the above explanation.

In contrast to PEO, the solubility of PPO in water is much poorer. For example, PPO400, a very short polymer, is water-insoluble in a rather wide concentration range when the temperature is higher than about 325 K. Fig. 6 shows the calculated binodal and spinodal and experimental point for the H_2O–PPO400 system. Good agreement is obtained.

It has been mentioned previously that changes in the molecular weight or the ratio of EO to PO can influence the LLE of H_2O–EOPO systems. In this study, EOPO contains 50% EO and 50% PO, while PEO and PPO are taken as copolymers with a molar ratio of 100% EO and 100% PO, respectively. Fig. 7 shows the influence of the molecular weights and the ratios of EO to PO on the binodals of the above three water–polymer systems. First, it can be found from Fig. 7 that the two-phase region of the water–polymer system expands with an increase in polymer molecular weight. For example, the loop of curve ¢Ù (PEO2270) is larger than that of curve ¢Ú (PEO2180), and the loop of curve ¢Û (EOPO4000, M_n=3640) is larger than that of curve ¢Ü (EOPO2000, M_n=2340). Second, the M_n of PEO2270 is very close to that of EOPO2000. However, from Fig. 7, it can be seen that the LCST of PEO2270 (M_n=2270) is higher than that of EOPO2000 (M_n=2340). The miscibility loop of PEO2270 (curve ¢Ù) is smaller than that of EOPO2000 (curve ¢Ü). This is due to PEO containing only the EO group. Moreover, the phase separation of PPO400 can occur at a relatively low temperature (325–425 K) and the two-phase region becomes very large (5–85% polymer, curve ¢Ý), but the copolymer contains

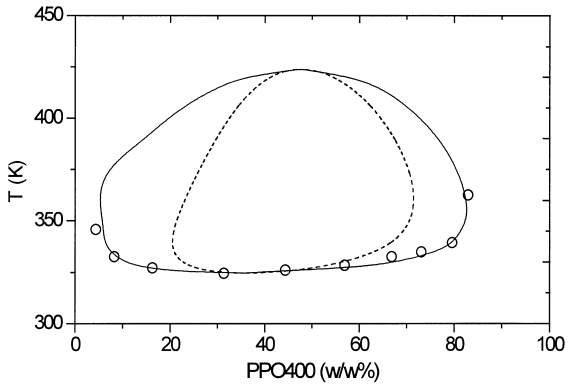

Fig. 6. Phase diagram for H_2O–PPO400 (M_n=400, r_2^0=13.2): (—) calculated binodal; (····) calculated spinodal; (○) experimental points — from Malcolm and Rowlinson [13].

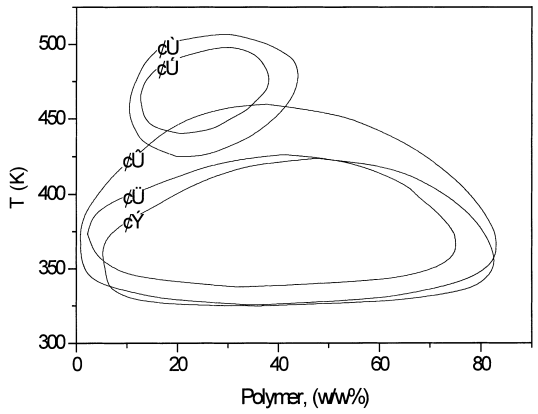

Fig. 7. The influence of molar ratios of EO to PO and M_n on the binodals of aqueous polymer solution. ¢Ù: PEO2270 (M_n=2270, 100% EO); ¢Ú: PEO2180 (M_n=2180, 100% EO); ¢Û: EOPO4000 (M_n=3640, EO/PO=1); ¢Ü: EOPO2000 (M_n=2340, EO/PO=l); ¢Ý: PPO400 (M_n=400, 100% PO).

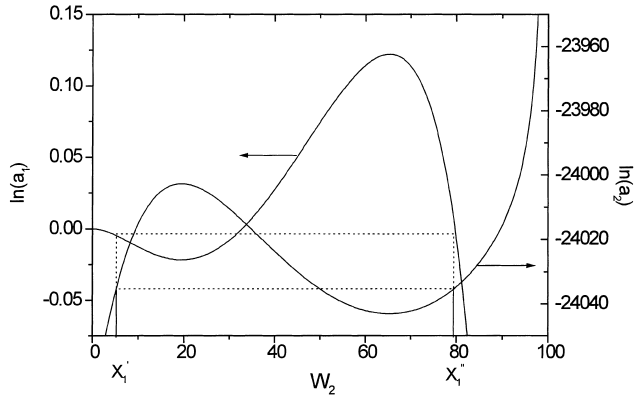

Fig. 8. Test of LLE — the calculated activities of H_2O and EOPO4000 with respect to the concentration (W_2) of EOPO at a temperature of 347.20 K.

only PO and the molecular weight is only 400. On the basis of the above discussion, it can be predicted that the binodal will move upwards and the miscibility loop will become small when the molar ratio of EO to PO increases under the same polymer molecular weight. The opposite change will take place with a decrease in the molar ratio of EO to PO. The prediction of this tendency is of great importance in designing and operating phase separation processes.

As an example for testing the calculated LLE, the activity–composition diagram of EOPO4000 is shown in Fig. 8. The phase equilibrium condition can be met when the two phases have the compositions X_1' and X_1'', respectively. The rectangular construction (dotted line) illustrates that, for phase compositions X_1' and X_1'', the activity of water is the same in both phases, and the activity of EOPO is also the same in the two phases. No other set of phase composition will satisfy the equilibrium.

5. Conclusions

Phase equilibrium data for H_2O–EOPO2000 and H_2O–EOPO4000 systems are obtained by determining the upper- and the lower-phase composition. Experimental results show that an increase in the molecular weight of EOPO can cause an expansion of the two-phase region and a decrease in the LCST.

The modified NRTL model is extended to describe the phase behaviour of water–polymer systems. A new adjustable parameter (c_r) is introduced into the calculation of LLE for the system having both LCST and UCST. Agreement between the calculated and experimental values is satisfactory for the three types of water–polymer systems with various ratios of EO to PO. The calculated results show that the binodal curves move upwards with an increase in the ratio of EO to PO or a decrease in the molecular weight. The two-phase region expands when the molecular weight of polymer increases or the ratio of EO to PO decreases.

6. Nomenclature

a	interaction parameter defined in Eqs. (3a) and (3b)
A	Helmholtz free energy
c_r	adjustable parameter for r_2
G	binary parameter in the NRTL equation
k	Boltzmann constant
M	molecular weight
N	number of molecules
q	effective segment number of polymer, or ratio of statistical degeneracies of two states
r	site-occupancy number per molecule
T	absolute temperature
X	effective mole fraction of segments
Z	coordination number in the lattice theory

Greek letters

α	non-random factor in the NRTL model
ϕ	volume fraction
τ	binary interaction parameter defined in the NRTL equation

Superscripts

0	pure state
$'$, $''$	upper and lower phases
(1), (2)	notation for distinguishment

Subscripts

NR	contribution from non-random mixing
i, j	any species or segment
ij, ii, jj	segment–segment pairs
1, 2	solvent and polymer, respectively

Acknowledgements

This research work is sponsored by the National Natural Science Foundation of China.

References

[1] P.A. Albertsson, Partition of Cell Particles and Macromolecules, 3rd Edition, Wiley, New York, 1986.
[2] H. Walter, D. Brooks, Partition in Aqueous Two-Phase Systems: Theory, Methods, Uses and Applications in Biotechnology, Academic Press, Orlando, FL, 1985.
[3] P.A. Alred, F. Tjerneld, R.F. Modlin, Partition of ecdysteroids using temperature-induced phase separation, J. Chromatogr. 628 (1993) 205–214.
[4] M. Li, Z.Q. Zhu, L.H. Mei, Partitioning of amino acids by aqueous two-phase systems combined with temperature-induced phase formation, Biotechnol. Prog. 13 (1997) 105–108.
[5] W. Li, Extraction of flavonoids from scutellaria by aqueous two-phase systems combined with temperature-induced phase separation, Ph.D. Thesis, Zhejiang University, Hangzhou, 1998.
[6] M. Li, Z.Q. Zhu, S.J. Yao, Separation of L-iso-leucine by aqueous two-phase system combined with temperature-induced phase formation, in: Proceedings of the Second China–Korea Conference on

Separation Science and Technology, Qingdao, China, 24–27 August 1998, pp. 534–538.
[7] J.M. Prausnitz, Molecular Thermodynamics of Fluid Phase Equilibria, Prentice-Hall, Englewood Cliffs, NJ, 1969, p. 240.
[8] R.P. Danner, M.S. High, Handbook of Polymer Solution Thermodynamics, American Institute of Chemical Engineers, New York, NY, 1993.
[9] T. Farkas, H. Stalbrand, F. Tjerneld, Partitioning of β-mannanase and α-galactosidase from Aspergillus niger in UCON/Reppal aqueous two-phase systems and using temperature-induced phase separation, Bioseparation 6 (1996) 147–157.
[10] S. Saeki, N. Kuwahara, M. Nakata, M. Kaneko, Upper and lower critical solution temperatures in poly(ethylene oxide) solutions, Polymer 17 (1976) 685–689.
[11] P.A. Alred, A. Kozlowski, J.M. Harris, F. Tjerneld, Application of temperature-induced phase partitioning at ambient temperature for enzyme purification, J. Chromatogr. 659(A) (1994) 289–298.
[12] H.O. Johansson, G. Karlstrom, B. Matttiasson, F. Tjemeld, Effects of hydrophobicity and counter ions on the partitioning of amino acids in thermoseparating Ucon-water two-phase systems, Bioseparation 5 (1995) 269–279.
[13] G.N. Malcolm, J.S. Rowlinson, The thermodynamic properties of aqueous solutions of polyethylene glycol, polypropylene glycol and dioxane, Trans. Faraday Soc. 53 (1957) 921–931.
[14] C. Bordier, Phase separation of integral membrane proteins in Triton X-114, J. Biol. Chem. 256 (4) (1981) 1604–1607.
[15] Y.T. Wu, Z.Q. Zhu, D.Q. Lin, L.H. Mei, A modified NRTL equation for the calculation of phase equilibrium of polymer solutions, Fluid Phase Equilibria 121 (1996) 125–139.
[16] P.J. Flory, Thermodynamics of high polymer solutions, J. Chem. Phys. 9 (1941) 660–661.
[17] M.L. Huggins, Solutions of long chain compounds, J. Chem. Phys. 9 (1941) 440.
[18] R. Kjellander, E.J. Forin, Water structure and changes in thermal stability of the system polyethylene glycol–water, J. Chem. Soc., Faraday. Trans. 77 (1981) 2053–2077.
[19] R.E. Goldstein, On the theory of lower critical solution points in hydrogen-bonded mixtures, J. Chem. Phys. 80 (1984) 5340–5341.
[20] G. Karlstrom, A new model for upper and lower critical solution temperatures in poly(ethylene oxide) solutions, J. Phys. Chem. 89 (1985) 4962–4964.
[21] W. Wang, D.A. Tree, M.S. High, A comparison of lattice-fluid models for the calculation of the liquid–liquid equilibria of polymer solutions, Fluid Phase Equilibria 114 (1996) 47–62.
[22] Y. Hu, H.L. Liu, D.S. Soane, J.M. Prausnitz, Binary liquid–liquid equilibria from a double-lattice model, Fluid Phase Equilibria 67 (1991) 65–86.
[23] M. Yu, H. Nishiumi, J.S. Arons, Thermodynamics of phase separation in aqueous solution of polymers, Fluid Phase Equilibria 83 (1993) 357–364.